A Phase Equilibrium Study of Cu-Fe Sulfides Between 700°C and 800°C

Laura Bilenker
Advisors: Dr. Philip Candela and Dr. Philip Piccoli
With Graduate Student Brian Tattitch
April 28, 2008
GEOL394

Abstract

The presence of small amounts of sulfide liquids in arc magmas has petrologic implications and applications for mineral exploration. Given that ore metals such as Ag or Au can partition into sulfide phases, small amounts of magmatic sulfides may "poison" ore formation. With the progressive crystallization of sulfides, the silicate melt becomes depleted in ore metals, and the probability of the formation of a hydrothermal ore deposit decreases. Sulfide melts, including potential Cu-Fe-S melts, may, because of the relaxation of crystal-chemical constraints, extract a greater proportion of ore metals from a melt.

There has been extensive research on the Cu-Fe-S system below 700°C. However, there are discrepancies regarding the presence of a liquid phase at 800°C in this system, and this problem was explored through sealed silica tube experimentation in this study. In the experiments, mixtures of sulfides, found not uncommonly in volcanic rocks, were heated to 750°C - 800°C. The run products were analyzed for the presence and composition of a melt, to determine the lowest temperature that sulfide liquid may exist in the Cu-Fe-S system. Methods of analysis include reflected light microscopy and use of an electron probe microanalyzer (EPMA). Compositions of the phases were plotted in Cu-Fe-S space.

First, an attempt was made to recreate the conditions and phase relations from Tsujimura and Kitakaze (2004) at 800°C. Toward this end, a mixture of bornite (Cu_5FeS_4) and chalcopyrite ($CuFeS_2$) was used. Optical observations along with imaging and compositional analyses from the electron probe microanalyzer show possible evidence of melt at this temperature. The bulbous shape, dendritic patterns, and presence of vesicles indicated that a melt phase was present at 800°C.

Subsequent runs were held for 3 days near 900°C before the temperature was lowered to between 700°C and 800°C, where the temperature was held for 3 more days. This way, the starting materials were conditioned to ensure homogeneity, which was lacking in the group 1 runs. Starting compositions of the runs included 60:40, 40:60, and 55:45 molar ratios of chalcopyrite to bornite, respectively, as well as combinations of chalcopyrite, bornite, and pyrrhotite. Run temperature for all of these experiments was between 800°C and 750°C.

Evidence of a liquid phase was identified in charges run at 800°C with starting compositions of about a 60:40 chalcopyrite to bornite molar ratio, and the resulting composition was between bornite and chalcopyrite. Many rounded vesicles and patterns of quenched liquid were seen in the runs of groups 1 and 2. This is consistent with Tsujimura and Kitakaze's 2004 findings.

No evidence of a quenched liquid phase was found by these methods in groups 3-9, which included the starting compositions previously mentioned run at 800°C and 750°C. Based on my observations in this project, a Cu-Fe-S liquid phase exists at temperatures down to at least 800°C, but does not appear to exist as low as 750°C. Mixtures of bornite and chalcopyrite, which are found in volcanic and plutonic igneous rocks, may, therefore, reflect the presence of melt, depending upon their composition, down to 800°C. These melts, if segregated, may affect the concentration of Ag, Au and other ore metals, in arc magmatic systems.

Table of Contents

Introduction

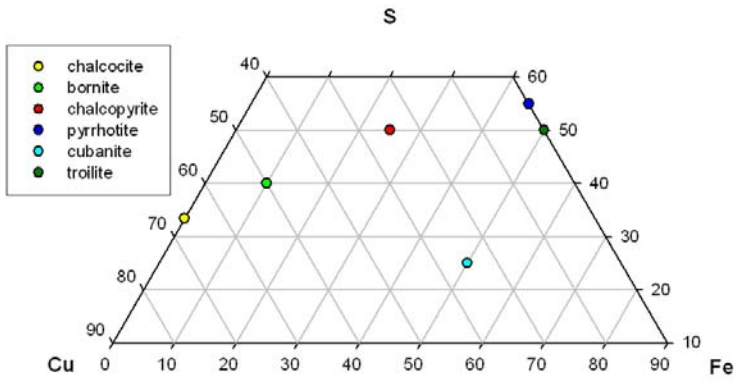

Figure 1: Approximate sulfide compositions

Whereas pyrite (FeS_2) is the most common sulfide in the Earth's crust, pyrrhotite ($Fe_{1-X}S$) is most abundant sulfide mineral in volcanic unaltered rocks. Traces of chalcopyrite ($CuFeS_2$) and bornite (Cu_5FeS_4) sometimes accompany, or occur instead of, pyrrhotite. Hattori (1999) suggests that such sulfides are ubiquitous in arc magmas, though in low modal proportions. Other sulfides include chalcocite (Cu_2S), cubanite ($CuFe_2S_3$), and troilite (FeS); the composition of these phases is plotted in Figure 1.

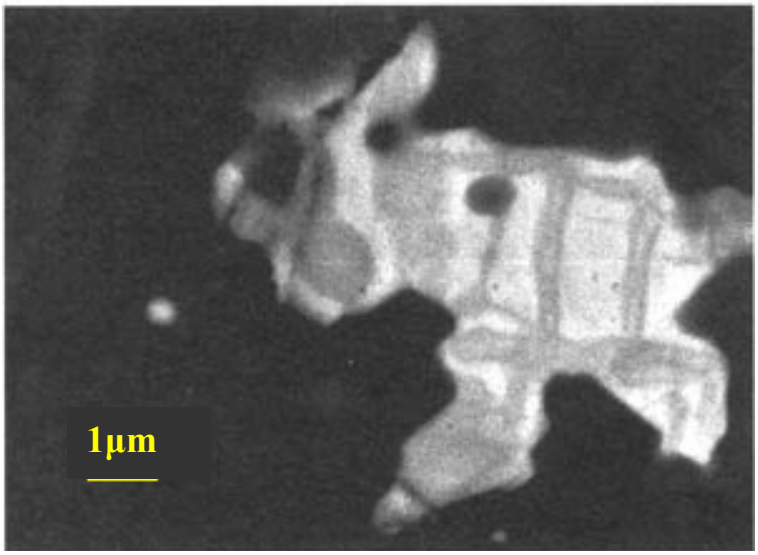

Figure 2: Backscatter electron image of a sulfide grain from Mt. Pinatubo (Hattori 1999).

At the time of eruption, sulfides exist as crystalline or molten phases. The magmatic temperature for intermediate to felsic igneous rocks can extend down to 650°C, the granite solidus at water pressures reflective of arc magmas (Holland 1967) (Appendix A). Evidence of the coexistence Cu-Fe sulfides at magmatic temperatures is seen in the products of the 1991 Mount Pinatubo eruption in the Philippines (Figure 2). In this backscatter electron image, the brighter areas are bornite, and the darker gray is chalcopyrite. The black background is epoxy. The pattern of the lines across this grain was interpreted by Hattori as the exsolution of chalcopyrite from bornite (1999). Hattori (1999) observed many samples with this same exsolution characteristic.

Many studies have been performed on the phase equilibrium of sulfides, and Kullerud was an early and major contributor (1969). In 2004, Tsujimura and Kitakaze revisited the system, and reported finding a liquid field stable 800°C that had not been previously observed in the extensive studies of Kullerud.

There are some inconsistencies in the literature about whether melting can occur along the degenerate bornite—chalcopyrite binary join within the Cu-Fe-S ternary at the temperature of eruption and crystallization of intermediate to felsic magmas. The phase diagrams in Figures 3-5 show only the midsections of the Cu-Fe-S phase diagram because no metallic Cu, Fe, or

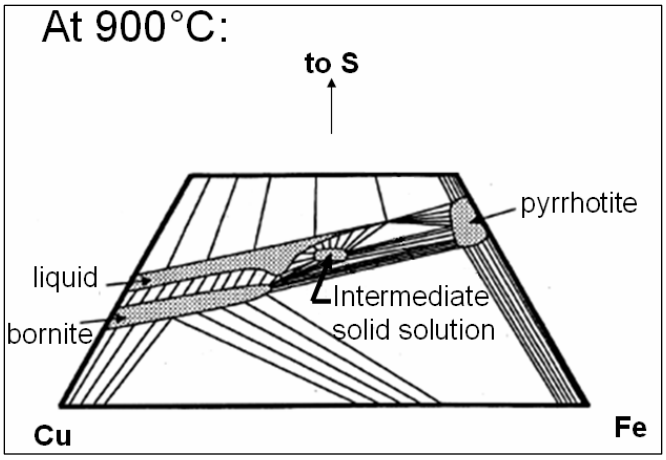

Figure 3: Cu-Fe-S phase relations adapted from Tsujimura and Kitakaze (2004)

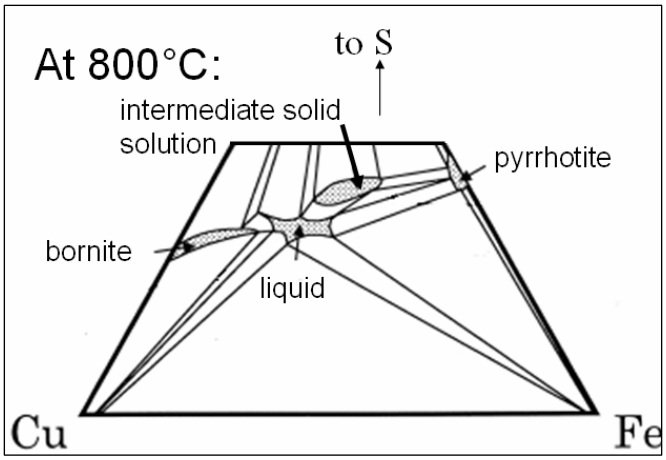

Figure 4: Adapted Cu-Fe-S system phase relations in atomic % by Kullerud et al. (1969) as redrawn by Tsujimura & Kitakaze (2004)

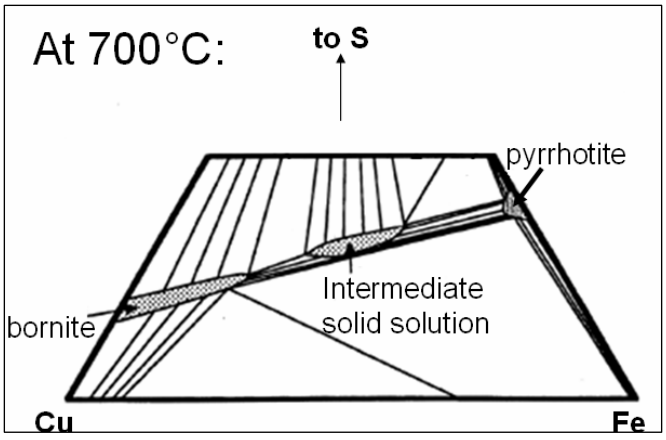

Figure 5: Adapted Cu-Fe-S system phase relations in atomic % by Kullerud et al. (1969) as redrawn by Tsujimura & Kitakaze (2004)

elemental S are found in common arc volcanic rocks at the time of eruption. Also, for the purposes of this research, intermediate solid solution (iss) labeled on the diagrams is the high-temperature form of chalcopyrite.

At 900°C, the three phase assemblage bornite-intermediate solid solution-pyrrhotite is stable (Figure 3). Also, the liquid field extends from the Cu-S constituent binary and past the center line that passes through the sulfur apex.

According to Tsujimura and Kitakaze, the bornite-intermediate solid solution tie line is severed and pyrrhotite coexists with liquid and intermediate solid solution at 800°C (Figure 4). Also, the liquid field is in a different location and a different size relative to Kullerud's 900°C isothermal section, and it is difficult to reconcile with their liquid field at that temperature. The liquid field reported by Tsujimura and Kitakaze occurs between the bornite and intermediate solid solution fields, partially extending above bornite and below intermediate solid solution. In addition, liquid coexists with pyrrhotite. Liquid may or may not be related to the liquid field present at 900°C, but the chemographic and phase equilibrium relations of the liquid fields is unclear: do the liquids lie on the bornite—chalcopyrite binary, or are they true ternary liquids? If this is the case, dropping in temperature has produced melt.

At 700°C, no liquid field is present (Figure 5). Also, although it is difficult to see in this diagram, there is a three-phase field between bornite, intermediate solid solution, and pyrrhotite similar to the phase relations at 900°C.

In this project, I address and explore this inconsistency by designing experiments that

explore three hypotheses concerning phase relations between the temperatures of 800°C to 700°C in the Cu-Fe-S system: (1) liquid remains stable and a bornite-intermediate solid solution tie-line is established; pyrrhotite does not coexist with bornite; (2) liquid remains stable and the bornite-pyrrhotite tie-line is established; and (3) the three-phase assemblage bornite-intermediate solid solution-pyrrhotite is established and the liquid phase disappears, or becomes an interior phase.

It is important to address the previously mentioned discrepancy because there are important implications concerning ore metal partitioning. Metals such as Ag and Au are more likely to dissolve in molten Cu-Fe-S phases than bornite solid solution or intermediate solid solution due to crystal chemical limitations. If metals partition more strongly into the sulfides relative to the silicate melt, they are depleted in the melt with progressive crystallization. Therefore, the probability of hydrothermal ore formation decreases.

Competing hypotheses, like those of Core et al. (2006), suggest that hydrothermal ore formation would not be affected in this way. Identifying a significant amount of bornite and chalcopyrite in dikes at the Bingham porphyry deposit, they speculate that sulfides supply ore metals to the magma, rather than inhibiting ore formation. However, large amounts of sulfides are also lost at depth in the crust during the ascent of magma, while Core et al.'s observations are of more shallow condition (2006).

Experimental Design and Methods

This research comprised a series of laboratory experiments followed by optical and chemical analytical techniques. In sealed silica tubes, mixtures of common sulfides (Figure 6) are loaded into a furnace. The tubing used for the first set of runs had walls 1 mm thick around a hole about 2 mm in diameter. To decrease the amount of free space in the capsules, tubing with walls 2 mm thick and a 1.5 mm diameter hole was used in subsequent experiments. As previously mentioned, the temperature of interest could have reached as low as 650°C, but not much higher than 800°C, where Tsujimura and Kitakaze (2004) reported a previously undiscovered liquid field.

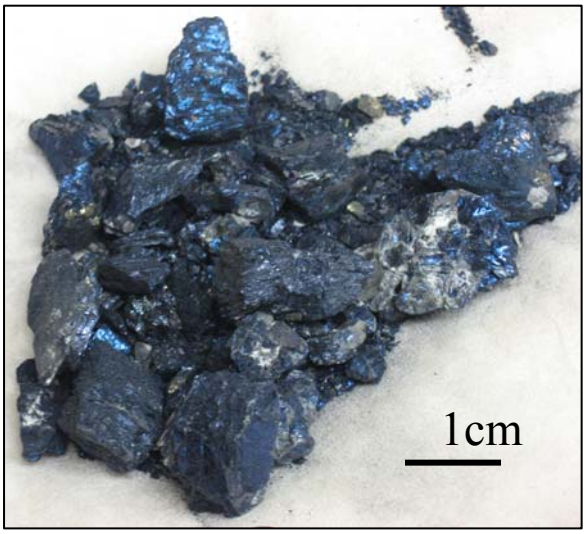

Figure 6: Starting bornite

The tubes were cut done by melting the glass with a flame produced from a burner fueled by methane and oxygen (Figure 7). The tubes were cut to approximately five inches in length and placed in an oven at around 115°C until the starting materials were prepared. Once cooled to room temperature, the tubes were filled with the dry sulfide mixture and covered with Parafilm to avoid contamination.

Initial experiments contain a binary mixture of bornite and chalcopyrite with replicates prepared for each molar ratio. The starting material used in the four tubes of the first experiment was close to Cu_2S (chalcocite) and $CuFeS_2$. The bornite used can be seen in Figure 6. The first experiments were conducted with molar ratios of approximately 60:40 chalcopyrite to bornite, or about (57% chalcopyrite to 43% bornite by weight). A table detailing starting composition ratios and other run information can be found in Figure 8. A Mettler AE240 was used and displays grams to the 10^{-5} decimal place. Based on repeated measurements, each mass could be determined to $\pm$0.00002g.

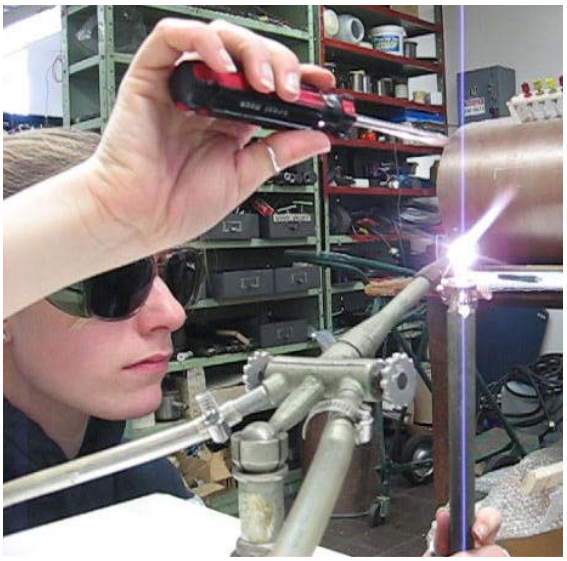

Figure 7: Sealing a silica tube

Experiments were labeled by group number and duplicate letter. For example, runs in group 2 had a 60:40 chalcopyrite to bornite starting mixture, and spent three days at 800°C after thermal conditioning. They are labeled A and B for ease of identification and specific measurements.

Run	Run Temperature (°C)	Run Time	Composition (molar ratio)	Furnace/Quench	Before Run Temperature...
1A	803	3 days	60cp:40bn	H/7 seconds	No preconditioning
1B	803	3 days	60cp:40bn	H/7 seconds	No preconditioning
1C	803	3 days	60cp:40bn	H/7 seconds	No preconditioning
1D	803	3 days	60cp:40bn	H/7 seconds	No preconditioning
2A	800	3 days	60cp:40bn	H/6 seconds	900 for 3 days
2B	800	3 days	60cp:40bn	H/6 seconds	900 for 3 days
3A	800	3 days	40cp:60bn	H/6 seconds	900 for 3 days
3B	800	3 days	40cp:60bn	H/6 seconds	900 for 3 days
4A	750	3 days	60cp:40bn	H/5 seconds	900 for 3 days
4B	750	3 days	60cp:40bn	H/5 seconds	900 for 3 days
5A	750	3 days	40cp:60bn	H/5 seconds	900 for 3 days
5B*	750	3 days	40cp:60bn	H/5 seconds	900 for 3 days
6A	800	3 days	55cp:45bn	V/rapid	913 for 3 days
6B	800	3 days	55cp:45bn	V/rapid	913 for 3 days
7A	800	3 days	37.5cp:25bn:37.5po	V/rapid	913 for 3 days
7B	800	3 days	37.5cp:25bn:37.5po	V/rapid	913 for 3 days
8A	752	3 days	60cp:40bn	V/rapid	903 for 3 days
8B	752	3 days	60cp:40bn	V/rapid	903 for 3 days
9A	752	3 days	1/3 po of group 7	V/rapid	903 for 3 days
9B	752	3 days	1/3 po of group 7	V/rapid	903 for 3 days

Key: orange: chalcopyrite-rich starting mixture
blue: bornite-rich starting mixture
green: pyrrhotite included in starting materials
5B*: dropped to the bottom of the furnace (~1 inch lower) at the start of run
H: horizontal furnace/slow quench
V: vertical furnace/instantaneous quench

Figure 8: Summary of run information details

Once starting materials were loaded, the tube was sealed. Making hooks on the ends of each of the tubes was not necessary, but was helpful for run identification and additional security in the furnace (Figure 9). This was done in the same way that the bottoms of the tubes were originally cut, with the addition of a vacuum seal for the duration of the procedure. The vacuum tube was attached to the open end of the capsule during the entire sealing process and was turned on very slowly to prevent any loss of material into the vacuum. Since experiments after runs 1A through 1D are thermally conditioned before run temperature, minor temporary heating of the charge should not have affected the outcome of the runs. The final lengths of the capsules were as short as possible, to minimize the amount of free space inside, following the experimental design of Tsujimura and Kitakaze (2004).

Another effort to more effectively recreate the work done by Tsujimura and Kitakaze (2004) at 800°C included conditioning the starting materials. The thermal conditioning technique used in these experiments did not exactly copy Tsujimura and Kitakaze, but the concept of conditioning before run temperature is what was important to ensure the homogeneity of the starting materials. They heated their experiments at a temperature below run temperature, removed them from the capsules, ground them, and loaded it all back into silica tubes to be sealed and run at a target temperature. There were a few advantages to conditioning the materials at a higher temperature rather than the procedure at a lower temperature. When the materials were run at a higher temperature, reactions happen faster and homogeneity can be achieved by bringing the materials to a temperature where it thoroughly mixed as liquid phases. Then, without removal from the furnace, they were run at the goal temperature. Significant time was saved by not opening capsules, grinding the materials, and then sealing new capsules.

Once the tubing was separated and effectively sealed, the tubes cooled to room temperature. Then, instead of simply melting away the sharpest pieces of the glass, a tool such as a flathead screwdriver was used to gently push the tip over itself into a hook. The hook not only aided in identification of the runs, but it provided extra security when binding the tubes for the furnace.

While the charges were inside of the furnace, it was crucial for each of the four capsules to be as

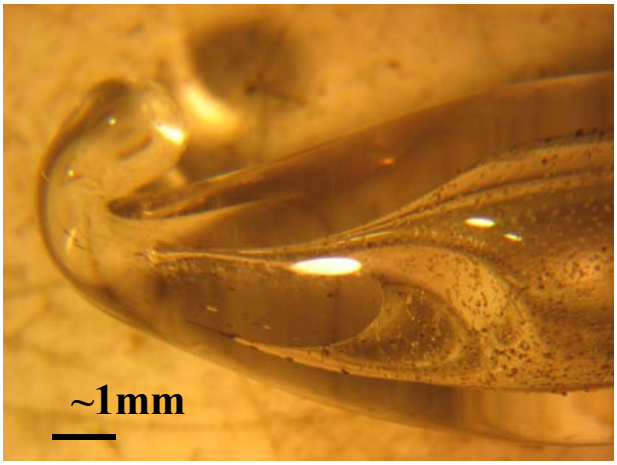

Figure 9: Example of a hook at the end of a vacuum sealed capsule (run 7A).

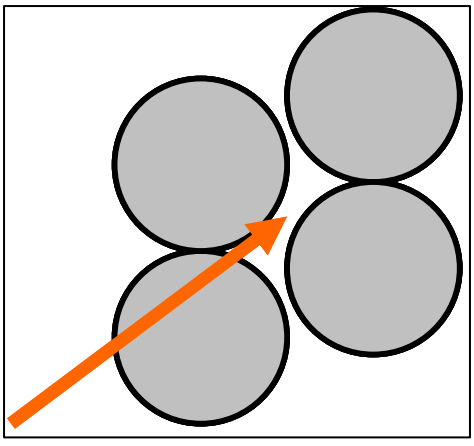

Figure 10: Schematic cross section normal to length of capsules. Orange arrow approximates location of thermocouple between 4 capsules.

close together as possible. This minimized temperature gradient and increased the accuracy of the temperature measurement. Four runs were bound together with Chromel P thermocouple wire using a tight figure eight pattern across the middle of each tube and through each hook. Temperature was measured during the run with a type-K Omega brand Ni-sheathed thermocouple which was secured to the bundle of capsules with the same wire. The thermocouple tip was placed between all of the tubes, as close to the center and as level with the materials as possible (Figure 10).

Figure 11: Vertical furnace set up

Experiments in groups 1 through 5 were run in a horizontal furnace in which there was a significant difference between temperature and the readout on the temperature controller. Therefore, in order to achieve 800°C inside, the furnace controller needed to be set at 668°C. Also, there was a "hot spot" approximately 25cm from the "door" of the chamber where the runs should be located (Mengason, personal communication 10/25/07). Additionally, there was a temperature gradient from the center of the furnace of approximately 1°C per centimeter (Mengason 10/25/07). The tubes should be maintained as vertical as possible for the duration of the experiment. The width of 4 runs bound together was about 2cm, and the temperature for each sample could vary by $\pm$2°C.

Experiments in groups 6 through 9 were run in a vertical furnace (Figure 11). The main difference between the set ups was the rate at which the run products are quenched. In the horizontal furnace, experiments were quenched manually in water, sometimes taking up to 7 seconds to reach room temperature. The quench process of the vertical furnace was practically instantaneous. A beaker was set up below the furnace so that, by snipping a wire, the capsules dropped into the water. It was important that the quenching process occurred as quickly as possible to avoid allowing the charges to cool and therefore crystallize with characteristics unlike those at desired the temperature.

The vertical furnace had two coils that control the internal temperature. A vertical furnace provides a conduit for free convection. Therefore, it was necessary that the charges be located at a spot that has the most stable temperature. In the particular furnace used for experiments 6 through 9, the hot spot occurred at a depth of 25 cm. Another note about this furnace is that the temperature tends to vary $\pm$2°C.

At the conclusion of the run, charges were removed from the capsule by first scoring the glass tube then exerting pressure with the thumbs to snap the tube open, or striking it carefully with a hammer to break it open. Some samples easily slid out of the tubing, but coaxing was occasionally necessary.

In group 1, two of the run products were mounted on a glass slide with carbon tape for energy dispersive spectroscopy (EDS) analysis on the JEOL 8900 SuperProbe. The other two run products were mounted in a round epoxy mount to be analyzed using wavelength dispersive spectroscopy (WDS) on the EPMA. The run products were also observed, sketched, and photographed under the reflected light microscope. Groups 2 through 9 were analyzed in a similar way, but EDS was not a primary method.

The Gibbs Phase Rule is useful for limiting the possible equilibrium outcomes of experiments. The rule states that the degrees of freedom (F), or the variance, for a particular composition in a system is equal to the number of components in the system (C), minus the number of phases (φ), plus 2 (Figure 12). Furthermore, if chemical variability is increased, a phase must be added, if the variance is to remain constant (Candela 2007).

$$F = C + 2 - \varphi$$

Figure 12: Gibbs Phase Rule

In the Cu-Fe-S system, there are 3 components: Cu, Fe, and S. That is, 3 constituents are required to define any composition for the whole system. So, $F = 3 + 2 - \varphi = 5 - \varphi$. The quartz tube used to hold the charges could be added as a component of the system during the experimental run. However, 1 component and 1 phase would be added which would not change the variance. For simplicity, the capsule will be ignored.

If the temperature is fixed at a predetermined value such as 800°C, then $F = 5 - 1 - \varphi = 4 - \varphi$ because 1 degree of freedom is used up. In groups 1, 2, 3, 4, 5, 6, and 8, conditions mimic a binary system since only bornite and chalcopyrite are used as starting materials and the run products only include bornite and chalcopyrite. Variance decreases again because the final phases have compositions along the join between those minerals. This is known as a colinearity. Now, $F = 3 - \varphi$.

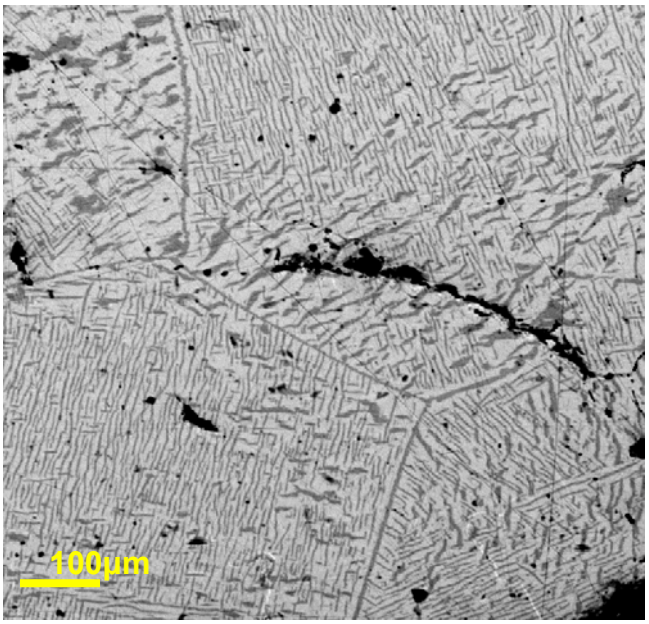

Figure 13: Run 6A, triple junctions

Therefore, the next question is: what is the maximum number of phases in the system at constant temperature? This will occur when there are no degrees of freedom, and $0 = 3 - \varphi$. Thus, $\varphi = 3$. Based on phase relations in the Cu-Fe-S system at these temperatures, there are 3 possibilities of what will be present

in the run products. S vapor is going to be one of the phases present. Evidence of this was observed in all runs as yellow crystals on the walls of the silica tubes after quench. Also, due to the colinearity, bornite and chalcopyrite will be the other 2 compositions possible. Also, a liquid phase may exist with a composition along the line. So, given the limitations imposed upon the system at equilibrium by the phase rule, we can expect the possible run products of such experiments to be: 1) bornite + liquid + vapor; 2) chalcopyrite + liquid + vapor; or 3) bornite + chalcopyrite + vapor.

The addition of pyrrhotite to the starting assemblage makes the system more complex. In that case, another phase is added, moving the system off of the colinearity, back to the ternary system, but the rule still works in a similar way.

This also raises the issue of equilibrium. Lengthy run times at thermal conditioning at a minimum temperature of 900°C help to ensure that samples reach equilibrium at run temperature, but there is also textural evidence in the run products that suggest they were at such conditions at run temperature. For example, at 800°C, run 6A exhibits what appears to be clear grain boundaries, known as triple junctions (Figure 13). The boundaries all meet with approximately equal 120° angles. Triple junctions like this suggest equilibrium without the presence of a melt phase (Figure 14) (Walte et al. 2007). This observation will be mentioned again later in the paper.

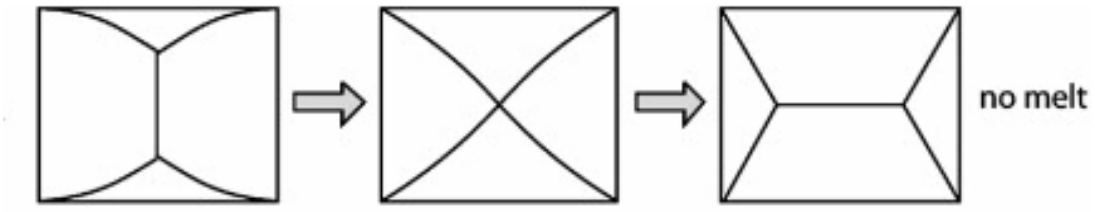

Figure 14: Shows topological changes without the presence of a melt (Walte et al. 2007).

Observations and Data

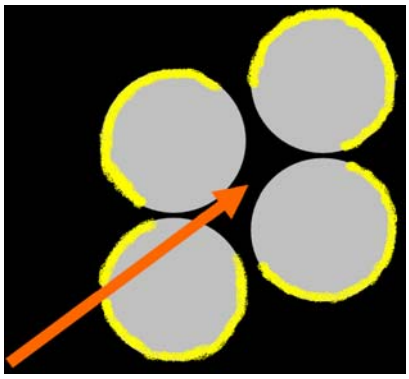

Figure 15: Sketch of portions of tube walls with yellow S crystals

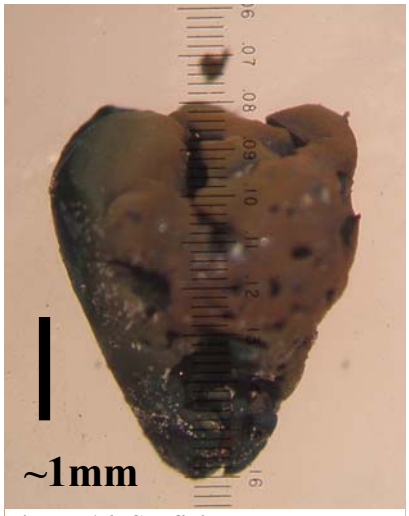

Figure 16: Surficial color differences in Run 1D

After the completion of the experiments, it was observed for every run that yellow sulfur crystals precipitated on the walls during the quench. This may be evidence of the presence of a vapor phase in the experiment. The crystals were concentrated on the sides of the tubes facing away from the center of the group during the time in the furnace (Figure 15). Also, this coating of crystals generally began distinctly above where the sulfide mixture resided at the bottom of the tube.

Group 1 run products were at the bottom of the tube as mainly one large, smooth and conical mass. The cone shape is dictated by the shape of the end of the silica tube where the materials sit. Any loose grains were hard to see, although there were a few. With the naked eye, it was difficult to see any separation of phases. However, under the microscope, it was easy to see that both 1C and 1D had one side with more of a rusty look to it, and the other side with a bluish tint (Figure 16). Also, all of the run products were very porous (Figure 17). The porosity may have been caused by the presence of sulfur vapor during the run. Pores, also referred to as vesicles, have been used in previous similar experiments as an indicator of a quenched liquid phase (Weidner 1984). Two morphologies are observed with the EPMA: liquid (Figure 17) and crystal (Figure 18). The smooth, round surface seen in Figures 16 and 17 is consistent with a liquid, and the angular crystal face characterizes crystal morphology (Figure 18).

Another feature to take notice of is the surface textures of the

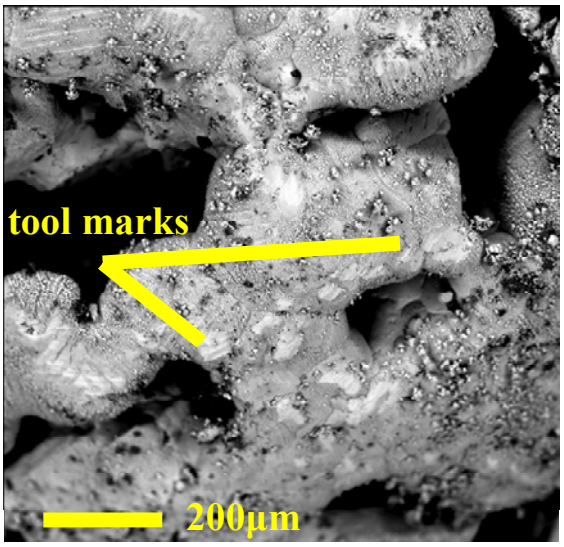

Figure 17: Backscatter electron image of the porosity of run 1C (liquid morphology)

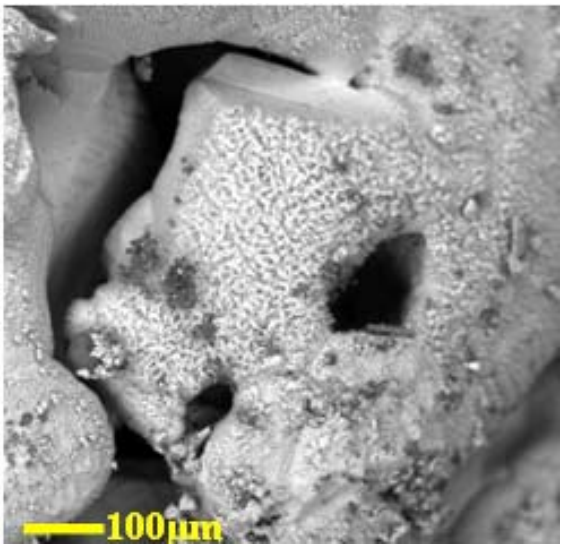

Figure 18: Backscatter electron images of bornite crystal morphology in run 1C

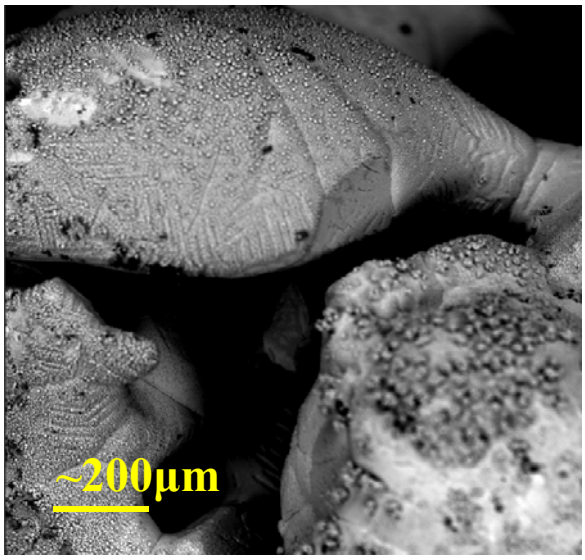

Figure 19: Backscatter electron image of the top left of 1C showing possible dendtritic quench structures and bulbous shape.

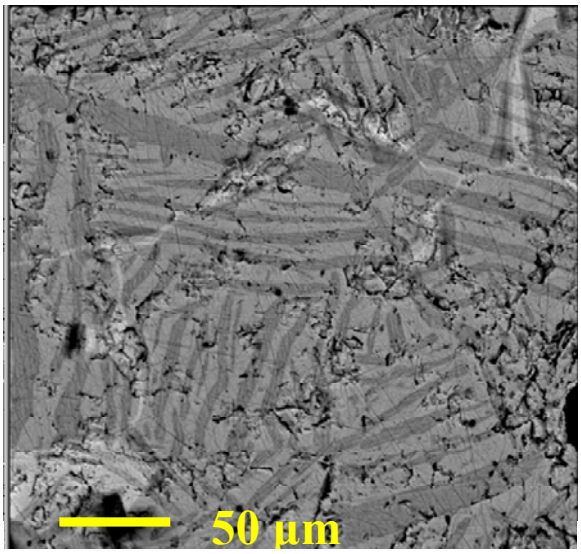

Figure 20: Dendritic pattern in run 1D

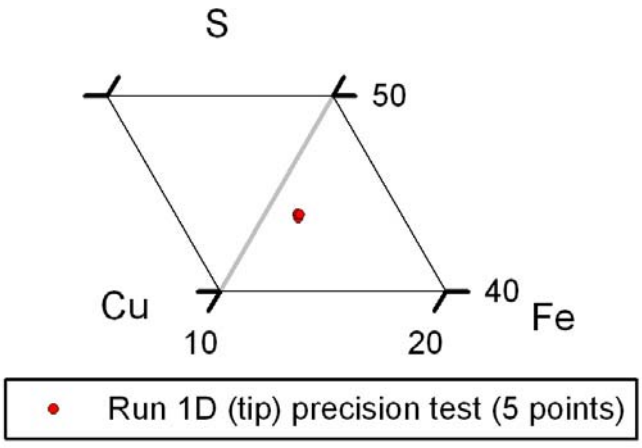

Figure 21: Precision test performed by WDS on Run 1D

run products. Many parallel structures, not due to tool marks, appear in the grains (Figure 19). It is possible that these structures formed upon quenching of a liquid phase. After mounting and polishing the samples to take a closer look with the EPMA, a different view of these textures can be seen in Figure 20. Keeping in mind that runs of group 1 were not thermally conditioned prior to run temperature, the bulbous shape, vesicles, and parallel surface textures serve as evidence of a liquid phase present at 800°C.

EDS analyses were also performed to estimate the chemical composition of the run products. It was difficult to get unambiguous results from EDS due to the nature of the samples. Their conical shape and large size cause much of the top portion and right side of both 1C and 1D to be blocked from the detector. However, a number of readings allowed us to see some contamination of the starting materials. For example, at the tip of the product, there was a dark gray, platy mineral with Na, Al, Si, and O. Although the starting materials were hand-sorted to remove any obvious contamination, particles may have been too small to see even under the microscope.

The presence of elements other than Cu, Fe, or S in the starting material that can dissolve in sulfide liquid has the potential to lower the melting temperature. However, this minor contamination should not produce any effect. Elements such as Al, K, Si, Mg, Na, and Ca do not typically go into sulfide liquids. They prefer silicate phases. On the other hand, Mn, Ni, Co, Pb, Zn, and Ag can affect the melting temperature.

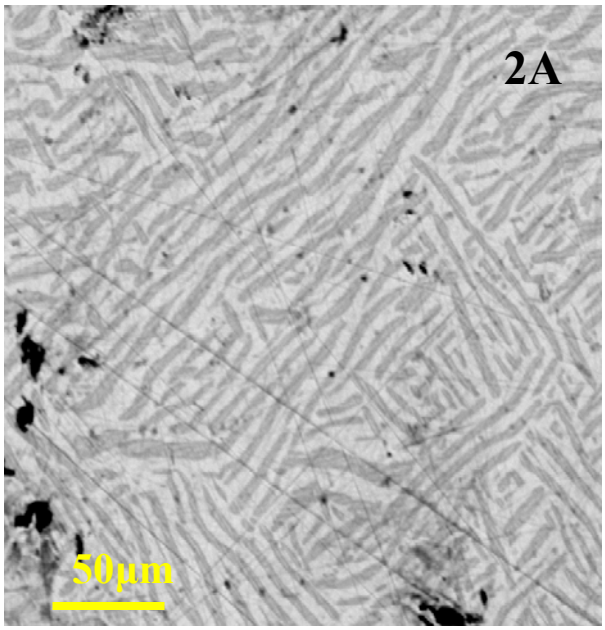

Figure 22: Lamellae of run 2A, similar to those of run 1D (Fig. 20)

In addition to EDS analyses, WDS was also performed. Results showed that the average composition of the 1C and 1D run products is spread between the bornite solid solution and intermediate solid solution fields, implying that these phases coexist at 800°C.

Errors associated with the WDS technique occur for many reasons. For example, if the sample is not completely flat after polishing, the readings may be affected. In the case of sulfides, it is sometimes difficult to polish them well due to their physical characteristics. Also, before running the WDS analysis for a sample, standards are measured to have comparable values. The data that is then gathered from the unknown samples is based off of those values. If the wrong standards are used, then the new data will not be accurate. The standard used for runs 1C and 1D was chalcopyrite.

Figure 23: Vesicles seen in run 2A

Precision of the WDS analyses was evaluated by repeatedly measuring the same spot five times on one sample. As you can see in Figure 21, the EPMA data are very precise. Five data points were collected for one location. There does not appear to be much variation from the measured composition—perhaps less than one percent. Therefore, error related to the precision of these WDS data is small.

A similar approach was applied to the rest of the experimental groups. However, EDS analyses were only used as necessary, to identify a questionable composition during the EPMA session.

The group 2 runs (2A and 2B) were used as an opportunity make improvements to the experimental design to more accurately reproduce the data of Tsujimura and Kitakaze and the results from group 1.

Figure 24: Faceted cracks and absence of vesicles in run 3A

There are numerous similarities between the run products of groups 1 and 2, and the only significant difference between them is that group 2 was thermally conditioned at 900°C for three days before spending three days at 800°C. First, as seen in Figures 20 and 22, they both display lamellae of similar composition and size. Also, these run products contain many rounded vesicles (Figure 23).

Group 3 was also run at 800°C, but the molar ratio of starting materials was 40:60 chalcopyrite to bornite. The results of these 2 bornite-rich runs were dramatically different from the potential of liquid present in the chalcopyrite-rich groups 1 and 2 at 800°C. There is a lack of rounded vesicles in 3A and 3B, but an abundance of cracks (Figure 24). These features are faceted and more angular than any of the cracks that occur in groups 1 and 2. Based on these optical observations and the compositional information gathered from WDS, group 3 may be in the bornite solid solution field (Appendix B).

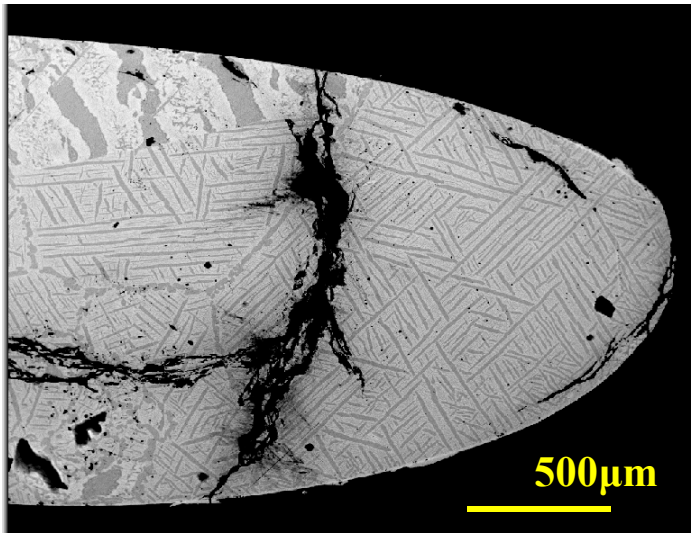

Figure 25: Run 4A--pegmatitic texture seen at the top left, surrounded by exsolution and a darker gray triple junction seen in the midsection, to the left of the large crack.

Group 4 was run at 750°C with a starting molar ratio of 60 chalcopyrite to 40 bornite. At 800°C, this mixture showed evidence of a liquid phase. However, at 50°C cooler, it seems that the melt no longer exists. Exsolution patterns are seen throughout the run products of group 4 (Figure 25). The tip of the products, the end that was facing downward in the furnace, appears to have a darker gray homogeneous region (Figure 26). The composition of this region plots close to the chalcopyrite region compared to the rest of the sample (Figure 27). This is interesting because bornite is denser than chalcopyrite. So, if these two solids coexisted, one might expect bornite to be on the bottom. However, since all runs approach the run temperature from 900°C, chalcopyrite probably crystallized first and sank to the bottom. The transition from the conditioning temperature to the run temperature in both of the furnaces used in these experiments lasted anywhere from five to thirty minutes, giving plenty of time for this to occur. Run 4A also

has a triple junction present, implying textural equilibrium, as well as crystal formation (Figure 25).

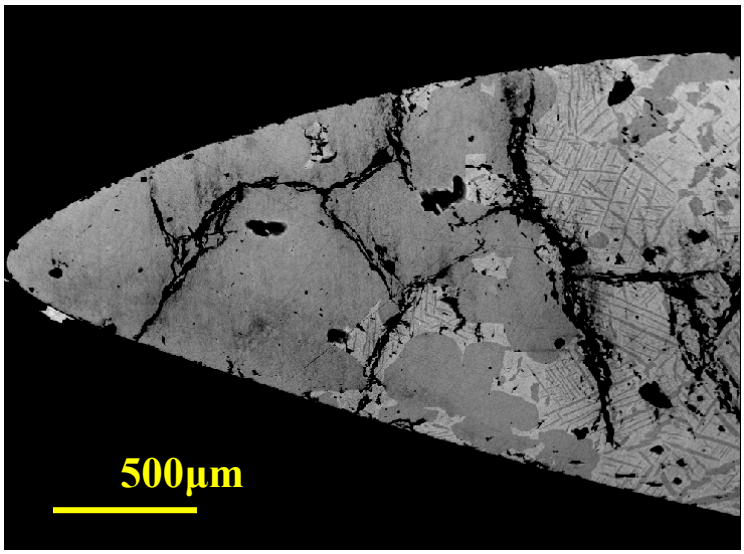

Figure 26: Tip of run 4A showing homogeneous chalcopyrite region

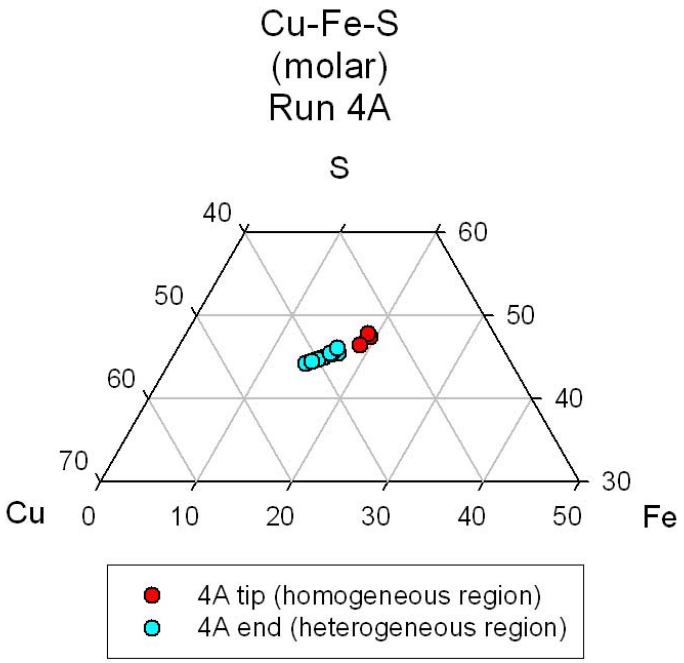

Figure 27: Plotted composition of run 4A tip and end based on WDS data.

Another interesting feature seen in 4A is a region of stripes of composition that are much larger than the "stripes" of the exsolution texture observed surrounding it (Figure 25). There are also spots of more chalcopyrite-rich areas near vesicles. One possible explanation for this is that larger crystals grew from the walls of the capsule, creating an experimental "pegmatite". Heat is lost more rapidly from the edges of an object, consistent with the fact that crystals would nucleate and grow in those regions.

60 moles of chalcopyrite to 40 moles of bornite was also the ratio of starting materials for group 8 experiments, which were run near 750°C as well. This duplication of group 4 conditions was an attempt to gain more insight into the complexities seen in those run products. 8A and 8B both had commonalities with 4A and 4B. For example, 8A displayed an exsolution texture with triple junctions. In 8B, a homogeneous, more chalcopyrite-rich region was seen in the tip with a heterogeneous, exsolved region above it (Figure 28). Also similar to 4A and 4B, "spots" with composition close to chalcopyrite were seen amidst the exsolution, near edges or vesicles left over from the preconditioning (Figures 28 and 29).

One possible explanation for the "spots" follows the idea of why the pegmatitic texture formed. Since the images produced by the EPMA are only showing one cut through the sample, it is possible that these spots

are actually crystals growing from another wall of the tube, toward the interior of the capsule. Also, many are found near vesicles that may have formed during the thermal conditioning stage (Figure 29). Therefore, another hypothesis regarding these features is that the vesicles provided quicker heat loss, and chalcopyrite was the first to crystallize, as seen in the tips of groups 4 and 8.

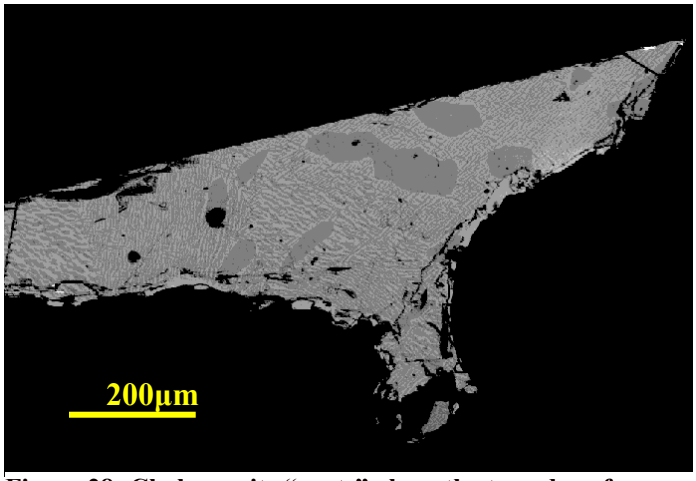

Figure 28: Chalcopyrite "spots" along the top edge of run 8A.

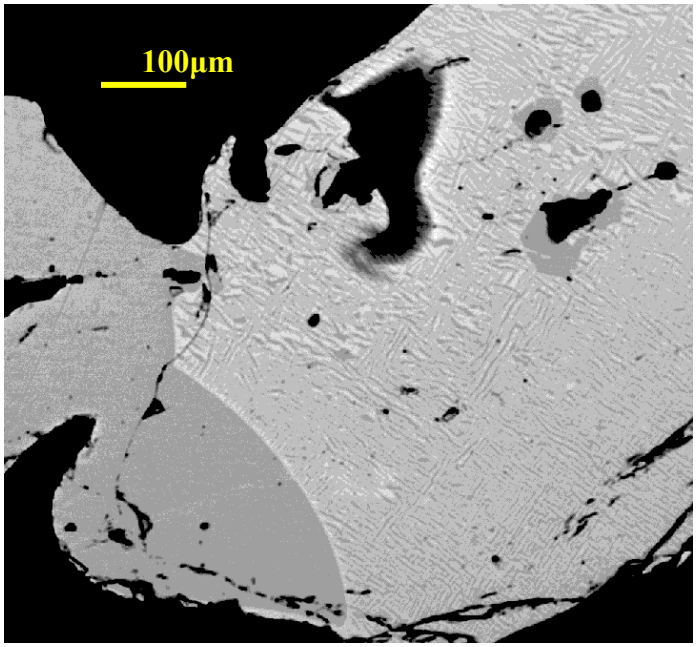

Figure 29: Divide between homogeneous chalcopyrite region and exsolution in run 8B.

In contrast to the complexities of groups 4 and 8, both runs of group 5 were homogeneous with many cracks running through them. Compositionally, the runs were close in composition to bornite (Appendix B). Combining these observations with those of group 3, it appears that a starting molar ratio of 40:60 chalcopyrite to bornite will produce charges that are in the bornite solid solution field at every temperature between 700°C and 800°C.

Group 6 started with a 55:45 molar ratio of chalcopyrite to bornite to target an area of the Cu-Fe-S phase diagram in which no run products had plotted yet. At 800°C with this starting composition, there is no evidence of the presence of liquid. Clear triple junctions along with deep cracks, a lack of vesicles, and a widespread exsolution pattern support this.

Pyrrhotite was added to group 7 with an approximately 37.5:25:37.5 molar ratio of chalcopyrite to bornite to pyrrhotite starting composition. The products of an 800°C run temperature are compositionally homogeneous. As seen in Figure 30, each point measured by WDS plots very closely to one another for both duplicates in this group. With the EMPA, thin white lines were seen throughout the products, interpreted to be grain boundaries and evidence of a solid phase since they are also seen in run 6B which also had exsolution textures and triple junctions.

The next pyrrhotite mixture included much less pyrrhotite; only 5mg of the overall ~35mg of starting material. These run products, 9A and 9B, also appeared to be compositionally

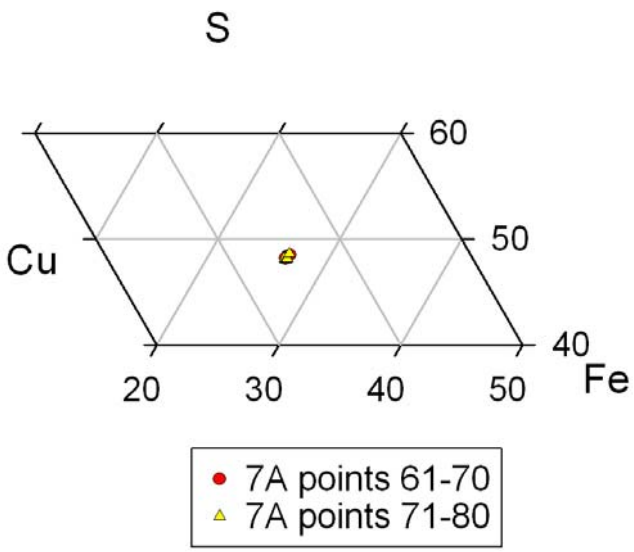

Figure 30: Phase relations of run 7A based on 20 points analyzed by WDS.

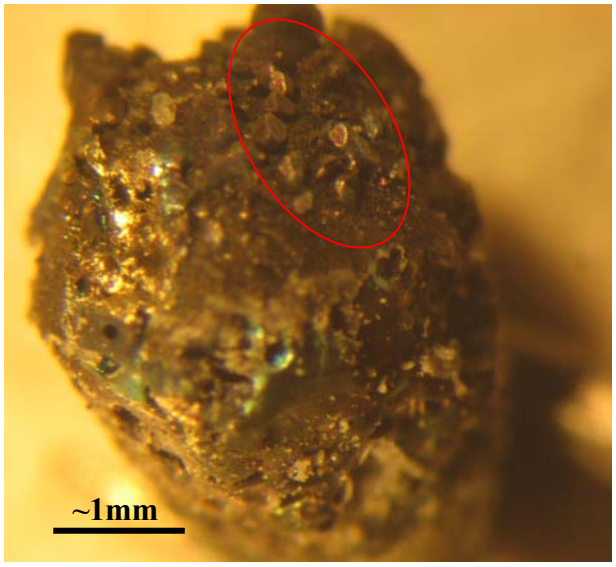

Figure 31: Crystal faces seen in run 7A, particularly visible within the red circle.

homogeneous. Under the reflected light microscope, group 9 runs showed defined crystal faces (Figure 31). Also, like group 7, it was seen with the EMPA that thin white lines seemed to outline grain boundaries. Therefore, in the groups containing pyrrhotite at both 800°C and 752°C, there was a lack of evidence of a liquid phase.

Plots of all run composition can be found in Appendix B.

Conclusions

I explored three hypotheses regarding phase equilibrium of Cu-Fe sulfides between 800°C and 700°C by performing a series of sealed silica tube experiments.

With decreasing temperature, my hypotheses include:

1. Liquid remains stable, a bornite-intermediate solid solution tie-line is established, and pyrrhotite does not coexist with bornite
2. Liquid remains stable and there is a bornite-pyrrhotite tie-line established
3. Bornite-intermediate solid solution-pyrrhotite coexist and the liquid phase disappears, or becomes an interior phase.

Nine experiments were completed, with seven different temperature-composition combinations, and 20 runs total. Once the experiments were performed and removed from the furnace, the run products were examined using various techniques, including analyses by reflected light microscope and electron probe microanalyzer (EPMA). These analyses were essential in determining whether there was melt present at a given temperature. Information gathered at the EPMA regarding the chemical composition of the products was used to plot the run products on a Cu-Fe-S phase diagram to illustrate phase relations as accurately as possible. A summary of the presence of each phase in each run, including whether a melt was present, can be seen in Figure 32. Also, Figures 33 and 34 summarize this information in Cu-Fe-S space.

Run	Bornite	Intermediate Solid solution	Pyrrhotite	melt	T (°C)
1A	√	√	-	√	803
1B	√	√	-	√	803
1C	√	√	-	√	803
1D	√	√	-	√	803
2A	√	√	-	√	800
2B	√	√	-	√	800
3A	√	√	-	-	800
3B	√	√	-	-	800
4A	√	√	-	-	750
4B	√	√	-	-	750
5A	√	√	-	-	750
5B	√	√	-	-	750
6A	√	√	-	-	800
6B	√	√	-	-	800
7A	√	√	√	-	800
7B	√	√	√	-	800
8A	√	√	-	-	752
8B	√	√	-	-	752
9A	√	√	√	-	752
9B	√	√	√	-	752

Figure 32: Summary of the presence of each phase in each run (check mark indicates that the phase was present, dash means it was not seen).

Backscatter electron images revealed quenched liquid patters in runs of groups 1 and 2, which started with a 60 to 40 molar ratio of chalcopyrite to bornite and spent three days at 800°C. Images of runs in groups with starting ratios of 40 chalcopyrite to 60 bornite mostly show homogeneity, at both 800°C and 750°C. Triple junctions in samples (groups 4, 6, and 8) served as

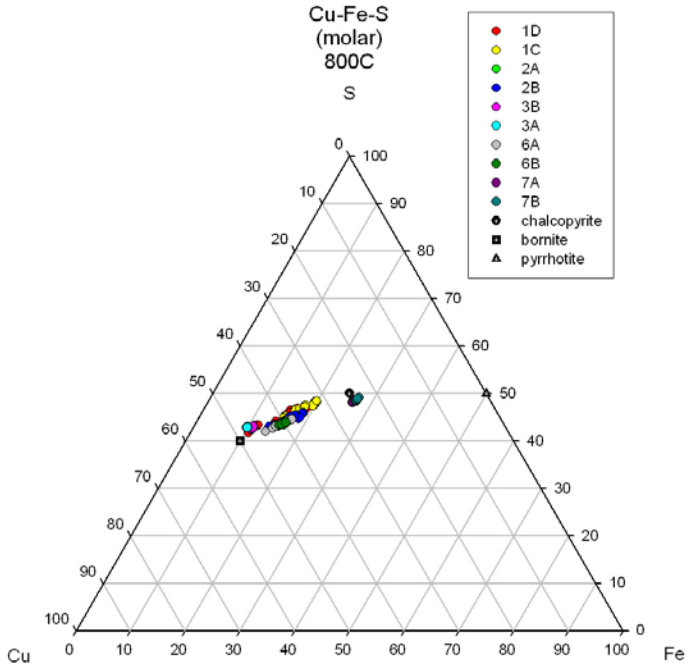

Figure 33: Ternary phase diagram including all experiments run at ~800°C.

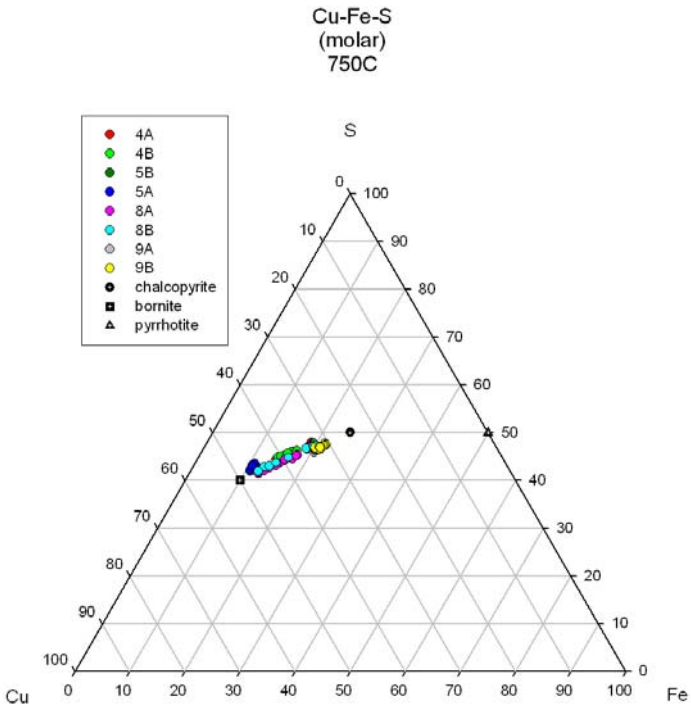

Figure 34: Ternary phase diagram including all experiments run at ~750°C.

evidence not only for a solid phase, but equilibrium as well.

Observations from the microscope include the porosity of runs in groups 1 and 2. The holes in these run products are rounded and abundant compared to some of the holes in group 3, for example, which are much more angular in general, and have many deep, faceted cracks. Figure 35 shows the plotted composition of the potential liquid field based on the most convincing evidence in the run products of groups 1 and 2. For example, data from the WDS analysis of regions 3 and 4 were used from 1C and 1D, but not the tip region and region 2 because there was concern regarding the heterogeneity of group 1. Contamination was discovered in the tip region, and crystal morphology was not seen as commonly toward the top of the run product.

Only the heterogeneous region of 2B was included in the estimation of the liquid field due to the presence of a large homogeneous region with composition close to chalcopyrite. The heterogeneous region consistently displayed dendritic textures and vesicles, while the homogeneous region did not.

Hypotheses #1 and #2, that the liquid remains stable as temperature drops from 800°C to 750°C, does not seem to hold based on these experiments. I did not see evidence that there is a substantial liquid field at 750°C, but Tsujimura and Kitakaze's speculation that a sulfide melt exists at 800°C was confirmed. It is possible that the liquid field extends below 800°C, but probably not all the way to 750°C.

Hypothesis #3 holds because the three phase assemblage, bornite-intermediate solid solution-pyrrhotite was reestablished and no evidence of liquid was found in experiments with run temperatures around 750°C.

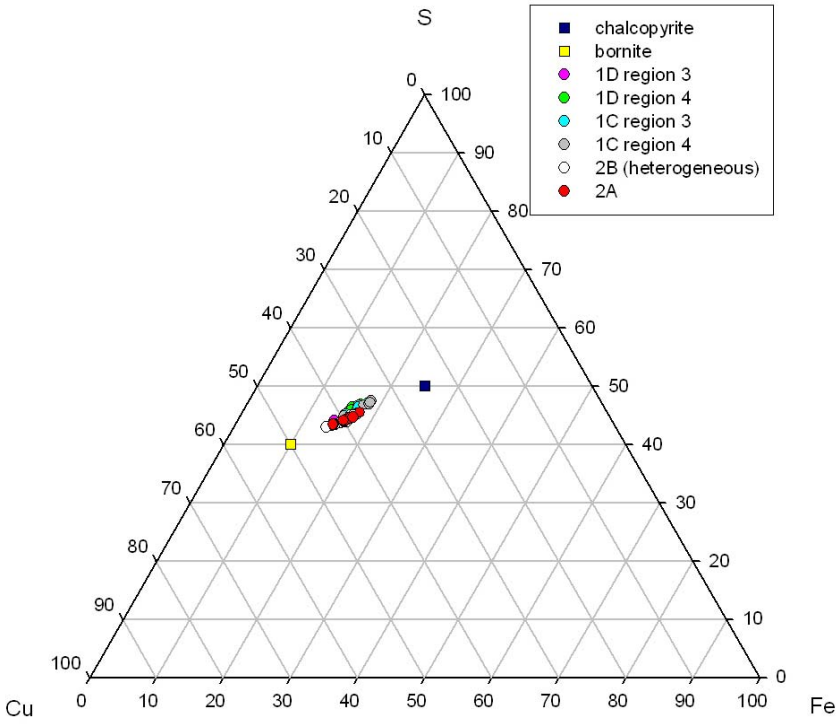

Figure 35: Potential liquid field at 800°C.

Suggestions for Future Work

There is much work related to this project that could be done. First, since I only had time to address temperatures of 800°C and 750°C, intermediate temperatures should also be explored to narrow down at what conditions the liquid field exists. Also, only two pyrrhotite combinations were used. Further investigation into starting compositions including pyrrhotite is also a possibility. Liquid was not identified during the 800°C run with pyrrhotite. Whether or not the liquid field disappears or becomes an interior phase (Hypothesis #3) would also be interesting.

Another area for future work might be to see what the highest level of oxidation of a magma is where a significant amount of bornite, intermediate solid solution, and sulfide melt exist. This would have implication for the formation of porphyry copper deposits.

Acknowledgements

First, I would like to thank my advisors Dr. Candela and Dr. Piccoli because your guidance and advice have been extremely helpful during the entire senior thesis experience. Dr. Piccoli, your help on the probe was also invaluable. I would also like to express gratitude toward Brian Tattitch for being so patient and giving of your time while I took time to learn the ropes. You

helped me learn a lot of ropes. Michael Mengason, you were also a big help by being available for the little questions I had and for generously sharing the furnace with me.

I would also like to take this opportunity to thank my awesome parents. The support that you have given me over the past 4 years has been absolutely incredible. No matter what, you've been right there, rooting for me the whole way and I am eternally grateful. You are a huge comfort, even when you may not realize that I need it. But mostly, thank you for humoring my dorkdom.

On a similar note, Zayde, I like that we can talk science and that you show a genuine interest in what I've done as a geology major. You are a wonderful role model in many ways. Don't worry; I will never let anyone hold cock fights in my lab.

Last, but not least, Eugenia, Joey, and Andrew, my fellow seniors, thanks for being such characters this past year.

Bibliography

Audetat, A. & Pettke, T. (2006): Evolution of a Porphyry-Cu Mineralized Magma System at Santa Rita, New Mexico (USA), Journal of Petrology, v. 47, no. 10, p. 2021-2046.

Borrok, D., Kesler, K., & Vogel, T. A. (1999): Sulfide Minerals in Intrusive and Volcanic Rocks of the Bingham-Park City Belt, Utah, Economic Geology, v. 94, no. 8, p. 1213-1230.

Cabri, L.J. (1973): New Data on Phase Relations in the Cu-Fe-S system. Economic Geology, v. 68, no. 4, p. 443-454.

Candela, P. A. (1992): Controls on ore metal ratios in granite-related ore systems: an experimental and computational approach, Transactions of the Royal Society of Edinburgh: Earth Sciences, 83, 317-326.

Candela, P.A. (Oct. 2007)"Gibbs Phase Rule", lecture notes for Laboratory for Mineral Deposits Research.

Candela, P.A. & Piccoli, P.M. (2005): Magmatic Processes in the Development of Porphyry-Type Ore Systems. Economic Geology 100th Anniversary Volume, p. 25-37.

Candela, P.A. Personal communication. September 18, 2007.

Core, D., Kesler, S., & Essene, E. (2006): Unusually Cu-rich magmas associated with giant porphyry copper deposits: Evidence from Bingham, Utah. Geology, v. 34, no. 1, p. 41-44.

Hattori, K. (1996): Occurrence and origin of sulfide and sulfate in the 1991 Mount Pinatubo eruption products. http://pubs.usgs.gov/pinatubo/hattori/.

Holland, H.D. (1967): Gangue Minerals in Hydrothermal Deposits, Geochemistry of Hydrothermal Ore Deposits, Ed. Hubert Lloyd Barnes, New York: Holt, Rinehart & Winston, Inc., p. 382-432.

Imai, A., Listanco, E., & Fujii, T. (1999): Highly Oxidized and Sulfur-Rich Dacitic Magma of Mount Pinatubo: Implication for Metallogenesis of Porphyry Copper Mineralization in the Western Luzon Arc. http://pubs.usgs.gov/pinatubo/contents.html.

Kullerud, G., Yund, R.A. & Moh, G.H. (1969): Phase relations in the Cu-Fe-S, Cu-Ni-S, and Fe-Ni-S systems. Economic Geology Monograph 4: 323-343.

Kullerud, G. (1967): Sulfide Studies, ed. Abelson, P.H., Researches in Geochemistry, v. 2, p. 286-321.

Jugo, P.J., Candela, P.A., & Piccoli, P.M. (1999): Magmatic sulfides and Au:Cu ratios in porphyry deposits: an experimental study of copper and gold partitioning at 850°C, 100 MPa in a haplogranitic melt-pyrrhotite-intermediate solid solution-gold metal assemblage, at gas saturation. Lithos, 46: 573-589.

London, D. (1992): The application of experimental petrology to the genesis and crystallization of granitic pegmatites. Canadian Mineralogist, 30: 499-540.

Mengason, Michael (2007): Experimental Study of the Partitioning of Cu, Ag, Au, Mo and W Among Pyrrhotite and Immiscible Fe-S-O and Silicate Melts, Diss. University of Maryland, College Park.

Mengason, Michael. Personal communication, October 25, 2007.

Mungall, J., (2002): Roasting the mantle: Slab melting and the genesis of major Au and Au-rich Cu deposits. Geology, v. 30, no. 10, p. 915-918.

Nagaseki, H. & Hayashi, K. (2008): Experimental study of the behavior of copper and zinc in a boiling hydrothermal system. Geology, v. 36; no. 1; p.27-30.

Robb, Laurence. Introduction to Ore-Forming Processes. Oxford: Blackwell Science Ltd, 2005.

Simon, A.C., Pettke, T., Candela, P.A., Piccoli, P.M., & Heinrich C.A. (2007): The partitioning behavior of As an dAu in S-free an dS-bearing magmatic assemblages. Geochimica et Cosmochimica Acta, v. 71, p. 1764-1782.

Stavast, et al. (2006): The Fate of Magmatic Sulfides During Intrusion or Eruption, Bingham and Tintic Districts, Utah. Economic Geology, v. 101, p. 329-345.

Tompkins, A., Pattison, D., & Frost, B.R. (2007): On the Initiation of Metamorphic Sulfide Anatexis. Journal of Petrology, v. 48, 511-535.

Tredoux, M., et al. (1995): The fractionation of platinum-group elements in magmatic systems, with the suggestion of a noval causal mechanism. South African Journal of Geology, v. 98, issue 2, p. 152-167.

Tsujimura, T. & Kitakaze, A. (2004): new phase relations in the Cu-Fe-S system at 800°C; constraint of fractional crystallization of a sulfide liquid. –N. Jb. Miner. Mh. 2004 (10): 433-444; Stuttgart.

Walte, N.P., Becker, J.K, Bons, P.D., Rubie, D.C., & Frost, D.J. (2007): Liquid-distribution and attainment of textural equilibrium in a partially-molten crystalline system with a high-dihedral-angle liquid phase, Earth and Planetary Science Letters, v. 262, p. 517-532.

Weidner, J. (1984): Equilibria in the system Fe-C-O and the origin of native iron, Canadian Mineralogist, v. 22, part 2, p. 348-356.

Appendix A: Granite Melt Curve

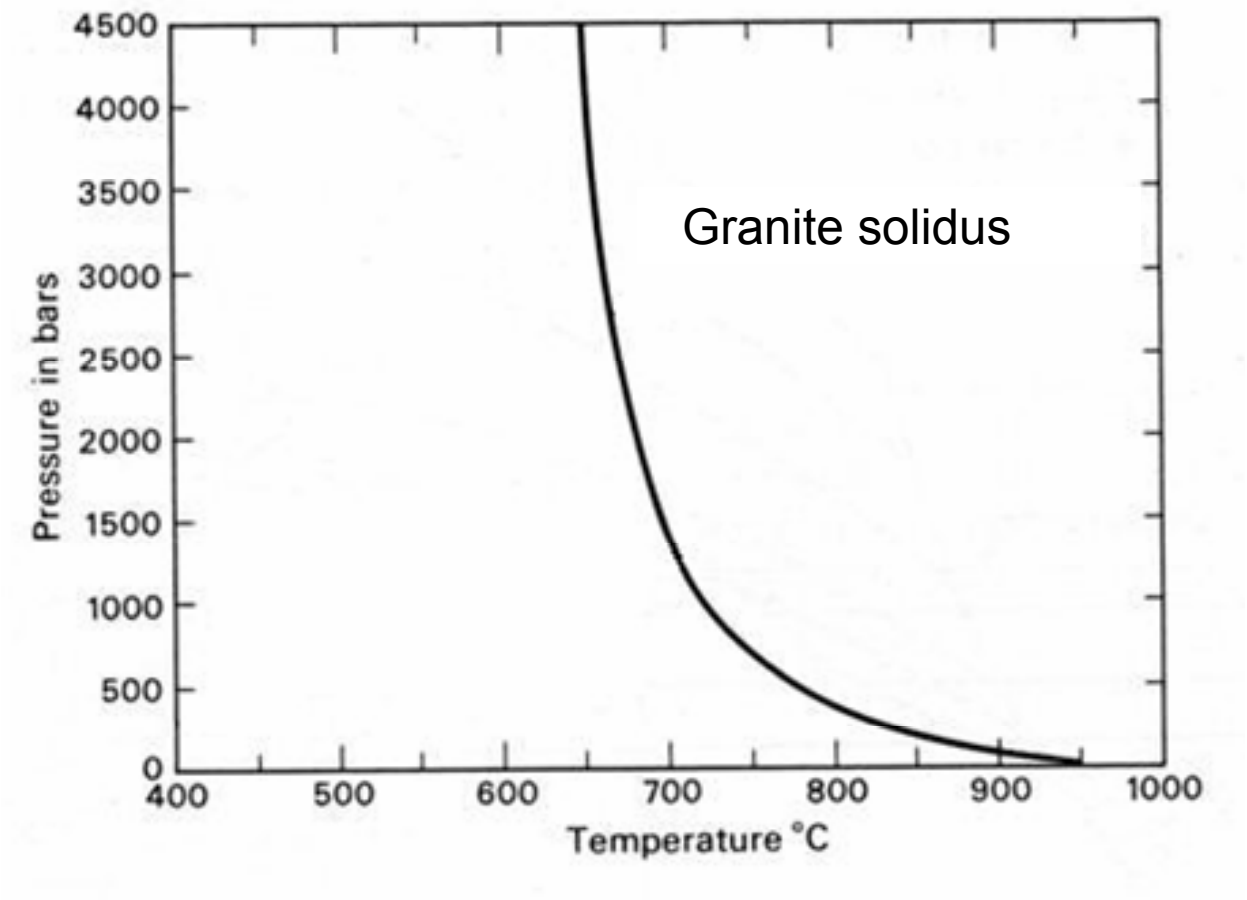

Granite melt curve adapted from Holland 1967.
Pressure on y-axis refers to water pressure because the granite solidus is vapor-saturated.

Appendix B: Phase Diagrams based on WDS data

800°C:

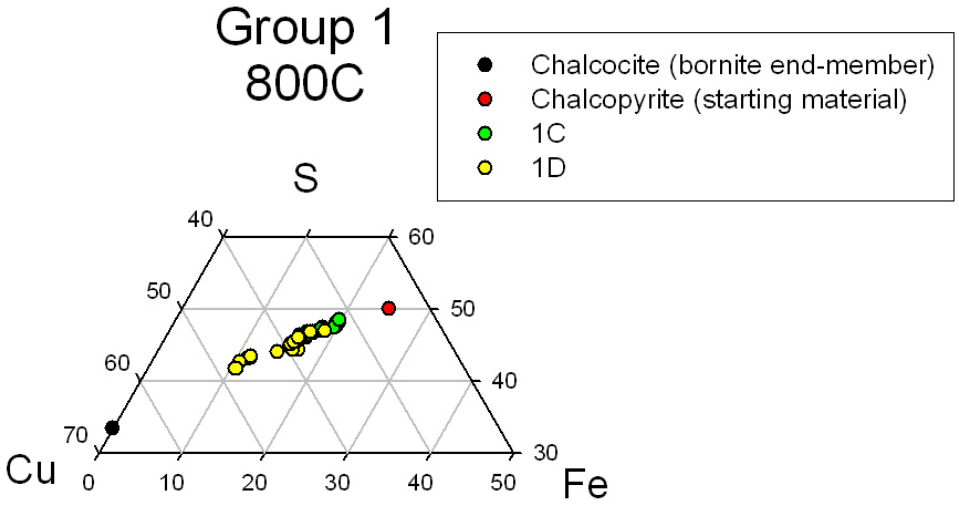

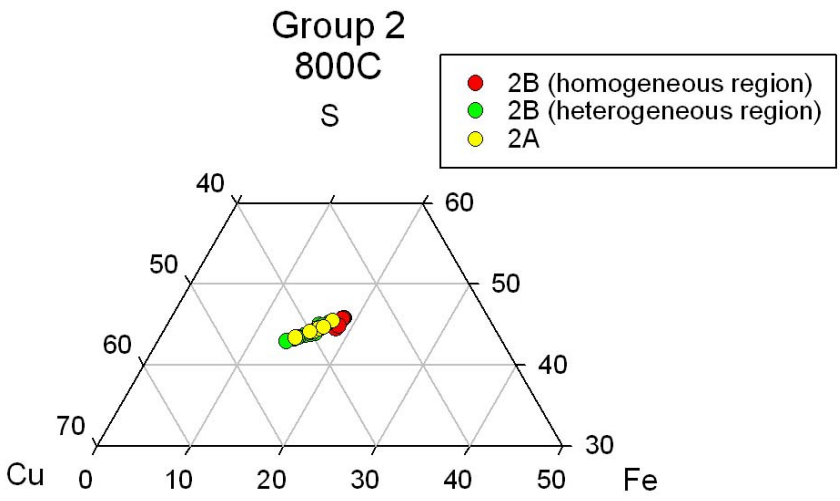

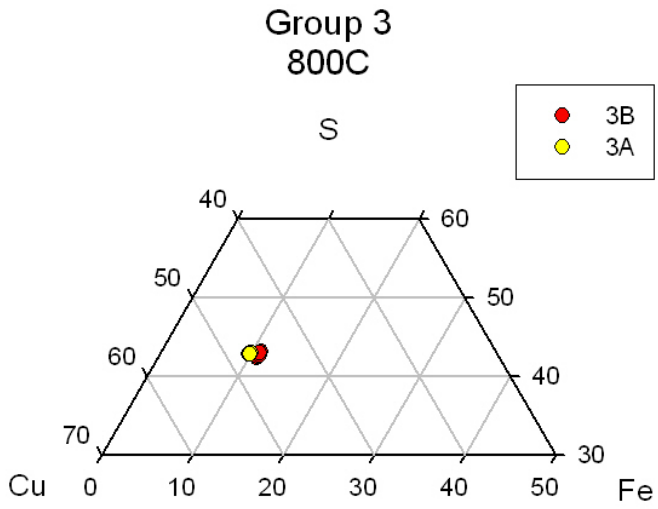
Group 3
800C
S
3B
3A
40
50
60
70
60
50
40
30
Cu
0
10
20
30
40
50
Fe

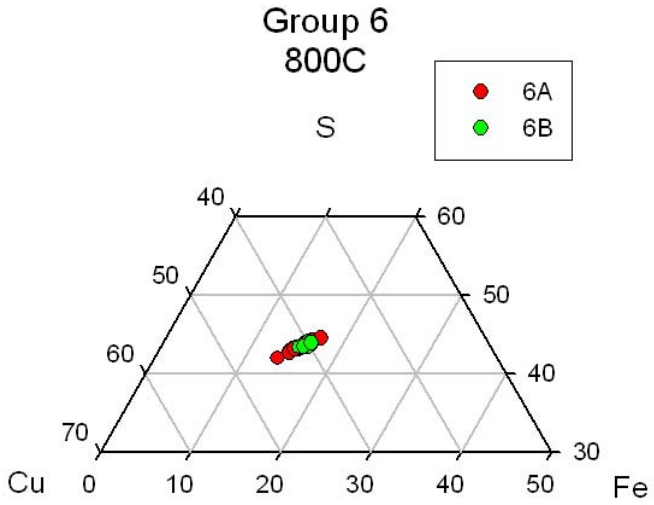
Group 6
800C
S
6A
6B
40
50
60
70
60
50
40
30
Cu
0
10
20
30
40
50
Fe

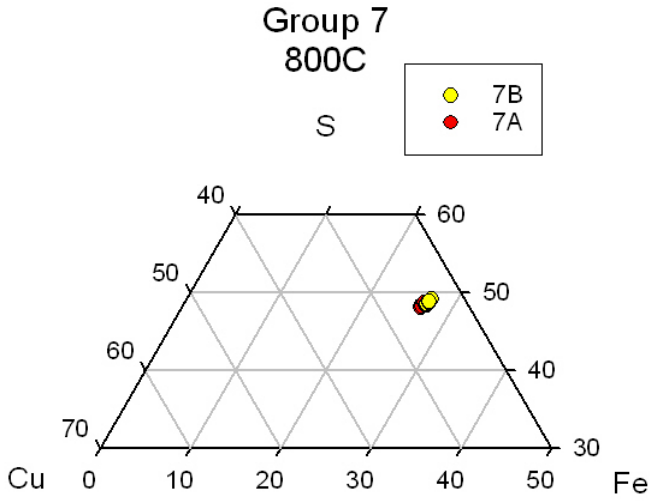
Group 7
800C
S
7B
7A
40
50
60
70
60
50
40
30
Cu
0
10
20
30
40
50
Fe

750°C:

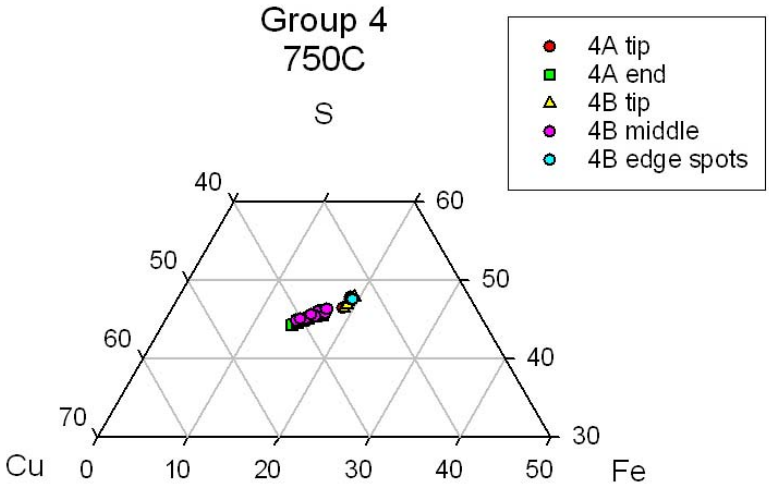
Group 4
750C
S
4A tip
4A end
4B tip
4B middle
4B edge spots
40
50
60
70
60
50
40
30
Cu
0
10
20
30
40
50
Fe

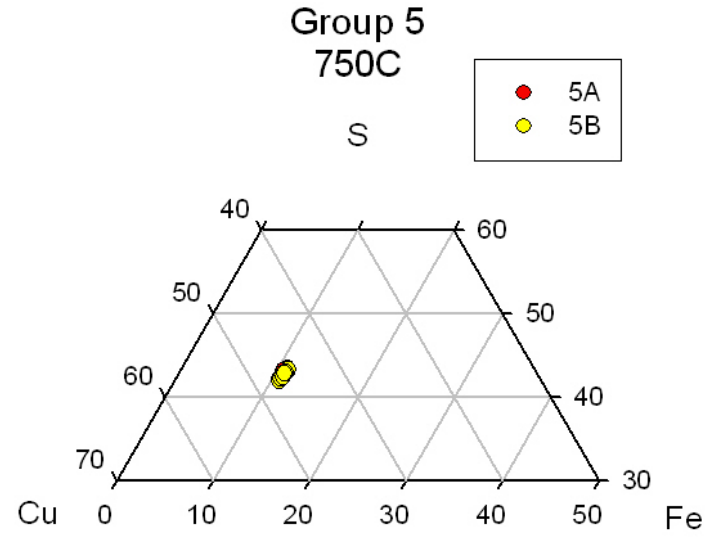
Group 5
750C
S
5A
5B
40
50
60
70
60
50
40
30
Cu
0
10
20
30
40
50
Fe

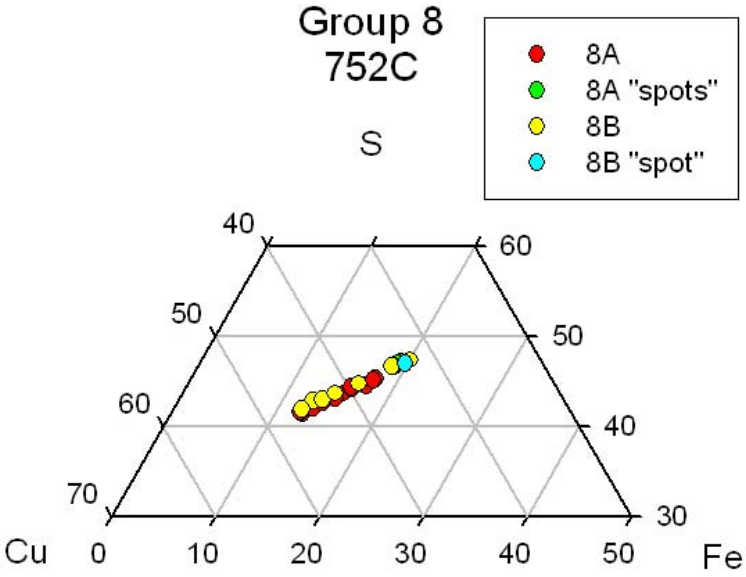
Group 8
752C
S
8A
8A "spots"
8B
8B "spot"
40
50
60
70
60
50
40
30
Cu
0
10
20
30
40
50
Fe

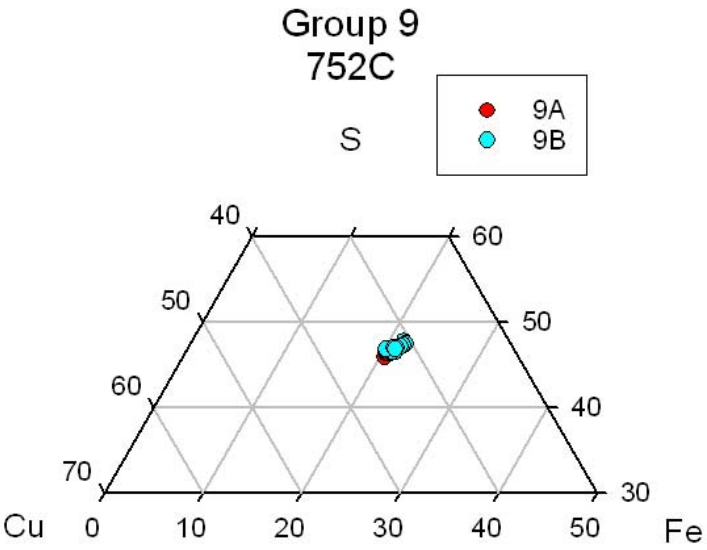
Group 9
752C
S
9A
9B
40
50
60
70
60
50
40
30
Cu
0
10
20
30
40
50
Fe

Appendix C: Honor Pledge

I pledge on my honor that I have not given or received any unauthorized assistance on this assignment.